Energy Band Structure of Copper*

GLENN A. BURDICK†‡
Massachusetts Institute of Technology Cambridge, Massachusetts
(Received 28 June 1962)

The $E(k)$ values were computed for the equivalent of 2048 points in the Brillouin zone and for energies ranging from the bottom of the 4*s*-band to approximately 2 Ry above the Fermi energy. From these calculations the Fermi energy, Fermi surface, and density of states were determined. Comparison of results with experiment shows not only qualitative but in most cases quantitative agreement. Agreement with recent independent theoretical work by Segall suggests an accurate solution of Schrödinger's equation for the potential used has been obtained.

INTRODUCTION

THE energy bands, Fermi surface, and density of states for copper have been determined by the augmented plane wave (APW) method. Since early 1954 the Solid-State and Molecular Theory Group (SSMTG) at the Massachusetts Institute of Technology has been engaged in programming the APW method for the digital computer.[1] This method was first proposed by Slater in 1937[2–4] and the results of the work described herein together with that of Chodorow on copper,[5] Saffren on sodium,[1] Wood on iron,[1,6] and Allen on potassium[1] give strong support to its being a very practical and accurate way of determining energy bands. The results for copper, in particular, demonstrate that energy-band calculations can agree quantitatively with experiment.

Copper has been the subject of considerable theoretical as well as experimental investigations. However, until quite recently there did not exist sufficient facilities, such as the APW digital computer program used in this work, to allow calculations to be made except at points of high symmetry in the Brillouin zone. As far as the author knows this work represents the most complete energy-band calculation made to date. One of the first calculations for copper was made by Krutter in 1935.[7] He used an extension of the Wigner-Seitz cellular method and concluded that the bands were quite free electron-like and obtained no overlapping of the "*s*" and "*d*" bands. Others using the cellular method with somewhat different potentials were Fuchs,[8,9] Tibbs,[10] and Howarth.[11] Chodorow's work in 1939[5,12] was the first application of the APW method. Fukuchi[13] used the orthogonalized plane wave method for copper in 1956. More recently Segall[14,15] has employed the Green's function method on copper. In the past, theoretical works on solids have been primarily restricted to intercomparisons of energy eigenvalues, their separations, their ordering, and similar general features of band structure; the reasons being that the $E(\mathbf{k})$ could be determined for only a few $\mathbf{k}$ of high symmetry. Furthermore, results obtained from theory could be compared to experiment in only the most general way (e.g., comparing *d* bandwidths with widths of x-ray emission spectra). In 1939, Rudberg and Slater[16] extended existing cellular method calculations to obtain an approximate density of states curve for copper. Beeman and Friedman[17] used this curve to make a qualitative comparison with their x-ray emission and absorption data for the *K* shell. They found quite good comparisons considering the necessarily sketchy data which could be used in determining the density of states. This will be discussed in greater detail later. The primary concern over past energy-band calculations (not only copper) was their inability to agree amongst themselves and the fact there had been only the most moderate success in being able to agree with experiment. Recent work in the SSMTG together with the work recently reported by Segall[14] and the work reported here seem to indicate that past difficulties lie in faulty potentials and/or computational errors and not in the energy-band theory itself.[18]

In the past, when $E(\mathbf{k})$ obtained in different studies have disagreed, it was not known whether the dis-

* This paper is a condensed version of the author's doctorate thesis submitted to the Massachusetts Institute of Technology in August 1961.

† Work performed while a National Science Foundation Fellow.

‡ Present Address: Sperry Microwave Electronics Company, Clearwater, Florida.

[1] Quarterly Progress Reports, Solid-State and Molecular Theory Group, April 15, 1954 to date (unpublished), contributions from D. J. Howarth, M. M. Saffren, J. H. Wood, and others; see: M. M. Saffren beginning with QPR, July, 1955 for work on sodium; L. C. Allen beginning with QPR, July, 1957 for work on potassium.

[2] J. C. Slater, Phys. Rev. **51**, 846 (1937).

[3] J. C. Slater, Phys. Rev. **92**, 603 (1953).

[4] M. M. Saffren and J. C. Slater, Phys. Rev. **92**, 1126 (1953).

[5] M. I. Chodorow, Ph.D. Thesis, M.I.T., 1939 (unpublished).

[6] J. H. Wood, Phys. Rev. **117**, 714 (1960); **126**, 517 (1962).

[7] H. M. Krutter, Phys. Rev. **48**, 664 (1935)

[8] K. Fuchs, Proc. Roy. Soc. (London) **A151**, 585 (1935).

[9] K. Fuchs, Proc. Roy. Soc. (London) **A153**, 622 (1936).

[10] S. R. Tibbs, Proc. Cambridge Phil. Soc. **34**, 89 (1938).

[11] D. J. Howarth, Proc. Roy. Soc. (London) **A220**, 513 (1953).

[12] M. I. Chodorow, Phys. Rev. **55**, 675 (1939).

[13] M. Fukuchi, Progr. Theoret. Phys. (Kyoto) **16**, 222 (1956).

[14] B. Segall, American Physical Society, annual meeting, New York, February 1–4, 1961 and meeting held in Washington, D. C., April 24–27, 1961; B. Segall and E. O. Kreiger, Bull. Am. Phys. Soc. **6**, 10 (1961). B. Segall, Phys. Rev. **125**, 109 (1962).

[15] B. Segall, General Electric Research Laboratory, Report No. 61-RL-(2785G), July, 1961 (unpublished).

[16] E. Rudberg and J. C. Slater, Phys. Rev. **50**, 150 (1936).

[17] W. W. Beeman and H. Friedman, Phys. Rev. **56**, 392 (1939).

[18] A joint paper by J. H. Wood, Jean Hanus, and the author discussing the dependence of energy bands on potential is presently being prepared for publication.

crepancies were due to differences in the crystal potential or to inaccuracies of either or both of the methods employed. Thanks to Segall's cooperation, pertinent information on this is now available. The extremely close agreement between his detailed calculations and the author's independent calculations using a different technique indicate that both techniques yield accurate solutions to the periodic potential problem. The very close agreement of these results and their agreement with experiment give us confidence that band structure studies like the present ones will be very useful in the understanding of many of the aspects of the electronic properties of solids.

As pointed out later, it has been possible to make a straightforward determination of the Fermi energy, Fermi surface, and density of states due to the large number of $E(\mathbf{k})$ values calculated. Segall did not calculate $E(\mathbf{k})$ at a sufficient number of general points to allow a determination of the density of states. However, he was able to calculate pertinent parameters of the Fermi surface by making use of two quite good approximations, the greatest inaccuracy being in his approximation of the volume inside the Fermi surface which he estimates to be in the range of 3–5%. The current work substantiates this estimate.

THEORY

Digital Computer Program

The digital computer program used to make the calculations in this report was provided by J. H. Wood who adapted M. M. Saffren's Whirlwind computer program to the IBM 704 and the IBM 709 computers. The program uses the Noumerov[19] method to integrate the radial wave equation and evaluates the Legendre polynominals and spherical Bessel functions in the standard manner by utilizing the various recurrence relations. Since the program has been thoroughly tested by Wood and utilized by several members of the SSMTG no detailed description as to the specifics of the program will be given. Perhaps the strongest support for its accuracy lies in the very close agreement of the results obtained by this program as compared to independent calculations by Chodorow[5] and Segall.[14,15]

APW Method

The APW method is due to Slater[2] and was modified slightly by Slater and Saffren.[3,4] The method as originally proposed by Slater is the one used in this work. For the sake of completeness a brief account of the method is now given. It is felt that a comprehensive treatment is unwarranted since such a treatment can be found in several works.[2–5,20,21]

[19] For a detailed account of this method, see G. W. Pratt, Phys. Rev. **88**, 1217 (1952).
[20] D. J. Howarth, Phys. Rev. **99**, 469 (1955).
[21] M. M. Saffren, Ph.D. thesis, M.I.T., 1959 (unpublished).

A necessary requirement for any method to yield good solutions to the electron in a periodic potential problem is that rapid convergence be obtained when the wave function is expanded in terms of the basis set being used. This criterion is obtained in the current method by expanding the wave function in terms of "atomic-like" functions within spheres centered about each nucleus and in terms of plane waves in the region between spheres. It is here assumed that the potential is spherically symmetric within the spheres and constant in the region between spheres. It is further assumed (although this assumption is unnecessary) that there is only one atom per Wigner-Seitz cell. As is well known, we need concern ourselves only with those space coordinates $\mathbf{r}$ restricted to the first Wigner-Seitz cell and with those wave vectors $\mathbf{k}$ restricted to the first Brillouin zone of reciprocal space since the wave functions must be of the form

$$\Psi_{\mathbf{k}}(\mathbf{r})=e^{i\mathbf{k}\cdot\mathbf{r}}w_k(\mathbf{r}), \tag{1}$$

where

$$\Psi_{\mathbf{k}}(\mathbf{r}+\mathbf{R}_j)=e^{i\mathbf{k}\cdot(\mathbf{r}+\mathbf{R}_j)}w_k(\mathbf{r})=e^{i\mathbf{k}\cdot\mathbf{R}_j}\Psi_{\mathbf{k}}(\mathbf{r}), \tag{2}$$

$\mathbf{R}_j$ being a lattice vector.

Choose a coordinate system whose origin is at the center of the first Wigner-Seitz cell and coincident with a copper nucleus. Let R represent one-half of the nearest-neighbor distance. Then for $|\mathbf{r}|\leq R$, the potential, say, $U(\mathbf{r})$ is spherically symmetric and the wave function can be put in the form

$$\Psi=\sum_{l=0}^{\infty}\sum_{m=-l}^{l}A_{lm}P_l^{|m|}(\cos\theta)e^{im\phi}u_l(r). \tag{3}$$

Here $u_l(r)$ satisfies the equation

$$-\frac{1}{2}\frac{d}{dr}\left(r^2\frac{du_l}{dr}\right)+\frac{l(l+1)}{r^2}+U(r)u_l=Eu_l, \tag{4}$$

and is to be regular at the origin (unlike the atomic case, being regular at infinity is not required). In the remaining region of the Wigner-Seitz cell the potential is assumed constant and any function of the form $e^{i\mathbf{k}\cdot\mathbf{r}}$ satisfies the Schrödinger equation. Now we use the well-known expansion for $e^{i\mathbf{k}\cdot\mathbf{r}}$ and obtain

$$e^{i\mathbf{k}\cdot\mathbf{r}}=\sum_{l=0}^{\infty}\sum_{m=-l}^{l}(2l+1)i^l j_l(kr)\frac{(l-|m|)!}{(l+|m|)!}P_l^{|m|}(\cos\theta)\times P_l^{|m|}(\cos\theta_k)e^{im(\phi-\phi_k)}. \tag{5}$$

Here r, θ, ϕ are polar coordinates about the origin and θ_k, ϕ_k are polar coordinates giving the direction of the wave vector $\mathbf{k}$. The functions $j_l(kr)$ are spherical Bessel functions and satisfy the differential equation

$$-\frac{1}{r^2}\frac{d}{dr}\left(r^2\frac{dj_l}{dr}\right)+\frac{l(l+1)}{r^2}j_l=k^2j_l. \tag{6}$$

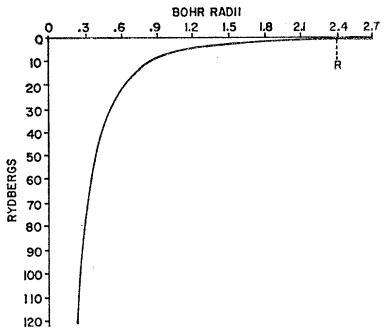

FIG. 1. Cu potential used for calculating wave functions.

The $P_l^{|m|}$ are the associated Legendre polynomials. In the reduced zone scheme which we have chosen, $\Psi_{\mathbf{k}}$ is a periodic but multiple-valued function of $\mathbf{k}$. Thus, if $\mathbf{k}_i=\mathbf{k}+\mathbf{K}_i$, where $\mathbf{k}$ is a wave vector restricted to the first Brillouin zone and $\mathbf{K}_i$ is a reciprocal lattice vector, then

$$\Psi_{\mathbf{k}i}=\Psi_{\mathbf{k}}. \tag{7}$$

In line with this, the natural choice of a basis set for expansion of a wave function with wave vector $\mathbf{k}$ is the set G_j, where G_j is given by Eq. (3) for $r\leq R$ and is $e^{i\mathbf{k}_j\cdot\mathbf{r}}$ for $r\geq R$. This G_j is made continuous at $r=R$ by comparing coefficients in Eqs. (3) and (5). We find that

$$A_{lm}{}^{i}=(2l+1)i^{l}\frac{j_l(k_iR)}{u_l(R)}\frac{(l-|m|)!}{(l+|m|)!}P_l^{|m|}(\cos\theta_i)e^{im\phi_i}. \tag{8}$$

Note, however, that the first derivative will not in general be continuous. See reference 2 for discussion of this aspect of problem. Expanding $\Psi_{\mathbf{k}}$ in terms of this basis set, we obtain

$$\Psi_{\mathbf{k}}=\sum_i a_iG_i,$$

TABLE I. Chodorow's potential energy for copper[a,b] (values are in atomic units).

r	$2Z_p(r)$	r	$2Z_p(r)$	r	$2Z_p(r)$
0.000	58.000	0.280	25.462	*1.02*	*6.567*
0.005	57.500	0.300	24.264	1.10	5.963
0.010	56.206	*0.340*	*22.186*	*1.18*	*5.429*
0.015	54.966	0.350	21.723	1.20	5.310
0.020	53.797	*0.380*	*20.470*	*1.26*	*4.983*
0.025	52.688	0.400	19.660	1.30	4.778
0.030	51.644	*0.420*	*18.851*	*1.34*	*4.573*
0.035	50.656	0.450	17.678	1.40	4.284
0.040	49.720	*0.460*	*17.308*	*1.42*	*4.197*
0.050	47.970	0.500	15.965	*1.58*	*3.594*
0.060	46.358	*0.540*	*14.772*	1.60	3.533
0.070	44.849	0.550	14.488	*1.74*	*3.183*
0.080	43.420	*0.580*	*13.625*	1.80	3.066
0.090	42.060	0.600	13.128	*1.90*	*2.874*
0.100	40.755	*0.620*	*12.631*	2.00	2.724
0.120	38.333	*0.660*	*11.680*	*2.06*	*2.635*
0.140	36.140	0.700	10.874	2.20	2.468
0.160	34.157	*0.780*	*9.408*	*2.22*	*2.446*
0.180	32.359	0.800	9.099	*2.38*	*2.293*
0.200	30.741	*0.860*	*8.252*	2.40	2.277
0.220	29.276	0.900	7.782	2.41	2.270
0.240	27.917	*0.940*	*7.312*	2.60	2.441
0.260	26.662	1.00	6.749	2.80	2.629

[a] Potential $=-2Z_p(r)/r$.
[b] Interpolated values are italicized.

where i ranges over all reciprocal lattice vectors. Applying the variational principle, we obtain the condition

$$\sum_j(H-E)_{ij}A_j=0, \tag{9}$$

where

$$(H-E)_{ij}=\int\Psi_i^*(H-E)\Psi_jdT, \tag{10}$$

which can be shown to be

$$(H-E)_{ij}=(\mathbf{k}_i\cdot\mathbf{k}_j-E)\left\{\delta_{ij}+\frac{4\pi R^2}{\Omega}\frac{j_1(|\mathbf{k}_j-\mathbf{k}_i|R)}{|\mathbf{k}_j-\mathbf{k}_i|}\right.$$
$$\left.+\sum_{l=0}^{\infty}(2l+1)P_l(\cos\theta_{ij})j_l(k_iR)j_l(k_jR)\frac{u_l'(R)}{u_l(R)}\right\}. \tag{11}$$

The problem then is to solve

$$\det|(H-E)_{ij}|=0. \tag{12}$$

The quantities $(H-E)_{ij}$ are implicit, as well as explicit, functions of the energy since the quantities $u_l'(R)/u_l(R)$ are implicit functions of the energy. For those $\mathbf{k}$ possessing symmetry the determinant will factor, resulting in considerable simplification for its solution.

Potential

The potential used for determining the energy eigenvalues for copper was derived by Chodorow.[5] This potential was arrived at by the addition of two potentials. The first potential is that potential which yields Hartree-Fock wave functions for $3d$ electrons when used in the Hartree equation; that is to say

$$V(r)=(\nabla^2\Psi/\Psi)+E, \tag{13}$$

where Ψ represents the Hartree-Fock wave function for $3d$ electrons in Cu^+. The second potential represents the Coulomb contribution of the $4s$ electrons. For this potential Chodorow used $4s$ wave functions determined from a previous cellular calculation due to Krutter.

It was necessary for the author to estimate the potential at certain points not given in Chodorow's numerical table. Chodorow's original potential plus the interpolated values are given in Table I. The sphere radius was taken to be half the nearest-neighbor dis-

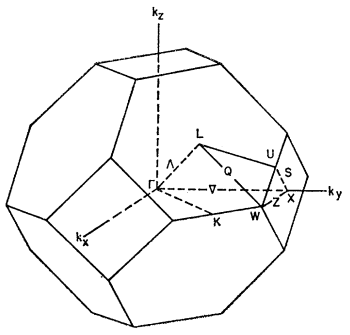

FIG. 2. The Brillouin zone for the face-centered cubic lattice.

TABLE II. Points of the first Brillouin zone for the fcc lattice.

BSW label	Order of the group of **k**	No. of like vectors	Wave vector **k**	BSW label	Order of the group of **k**	No. of like vectors	Wave vector **k**	BSW label	Order of the group of **k**	No. of like vectors	Wave vector **k**
Γ	48	1	000	Σ	4	12	440		2	24	441
Δ	8	6	010		2	24	450		1	48	451
Δ	8	6	020		2	24	460		1	48	461
Δ	8	6	030		2	24	470	Q	2	24	471
Δ	8	6	040	W	8	6	480		2	24	551
Δ	8	6	050	Σ	4	12	550		1	24	561
Δ	8	6	060		2	24	560	Λ	6	8	222
Δ	8	6	070		2	8	570		2	24	232
X	16	3	080	K	4	4	660		2	24	242
Σ	4	12	110	Λ	6	8	111		2	24	252
	2	24	120		2	24	121		2	24	262
	2	24	130		2	24	131		2	24	272
	2	24	140		2	24	141	U	4	8	282
	2	24	150		2	24	151		2	24	332
	2	24	160		2	24	161		1	48	342
	2	24	170		2	24	171		1	48	352
Z	4	12	180	S	4	12	181		1	48	362
Σ	4	12	220		2	24	221		1	24	372
	2	24	230		1	48	231		2	24	442
	2	24	240		1	48	241		1	48	452
	2	24	250		1	48	251	Q	2	24	462
	2	24	260		1	48	261		2	12	552
	2	24	270		1	48	271	Λ	6	8	333
Z	4	12	280		2	24	281		2	24	343
Σ	4	12	330		2	24	331		2	24	353
	2	24	340		1	48	341		2	12	363
	2	24	350		1	48	351		2	24	443
	2	24	360		1	48	361	Q	2	24	453
	2	24	370		1	48	371	L	12	4	444
Z	4	12	380		2	16	381				

tance or, what amounts to the same thing, the radius of the inscribed sphere in the Wigner-Seitz cell. A plot of the potential used is given in Fig. 1.

Face-Centered Cubic Lattice

The first Brillouin zone for the fcc lattice is shown in Fig. 2 and the various points of symmetry are labeled.[22] For the purpose of labeling points in the first Brillouin zone the factor $\pi/4a$ will frequently be dropped. Thus the wave vector $\mathbf{k}=(\pi/4a)(0,8,0)$ (which is the point labeled X in Fig. 2) will be written simply as (0,8,0) or even as 080 when there is no chance for confusion. The reason for this particular choice will become apparent somewhat later. The coordinates of the symmetry points as shown in Fig. 2 are

$\Gamma=000$; $\Delta=0x0$ where $0<x<8$

$X=080$; $\Sigma=xx0$ where $0<x<6$

$L=444$; $\Lambda=xxx$ where $0<x<4$

$W=480$; $Q=444+0x\bar{x}$ where $0<x<4$

$K=660$; $Z=x80$ where $0<x<4$

$U=282$;

$S=(2+x, 8, 2-x)$ where $0<x<2$.

A bar over a number in the above list is to be interpreted as a minus sign.

For the purpose of doing a complete determination of the energy band structure such that a reliable density of states curve and the topology of the Fermi surface could be obtained, the first Brillouin zone was partitioned into 2048 cubical volume elements. The energy eigenvalues were then computed for those **k** located at the center of each volume element. It is only necessary to compute the eigenvalues for those **k** lying in one forty-eighth of the Brillouin zone. From these, by the use of symmetry properties, the eigenvalues can be obtained for all 2048 points. The volume enclosed by the surfaces ΓLK, ΓKWX, ΓXUL, $LKWU$, and WXU (see Fig. 2) constitutes an appropriate one forty-eighth of the zone and 89 of the 2048 points used and the number of "like" points (or vectors) in the zone are listed in Table II. Thus, there is only one point "like" gamma, there are six points "like" 010. Here, **k** is said to be "like" **k** if

$$E_n(\mathbf{k}')=E_n(\mathbf{k}) \tag{14}$$

for all n, where n is an integer which labels the various energy bands. We shall use the usual convention and order the energies in such a way that

$$E_n(\mathbf{k})\leq E_{n+1}(\mathbf{k}), \tag{15}$$

the equality holding only in the event of degeneracy. The order of the group of the wave vector and the BSW label for symmetry points are also listed in Table II.

TABLE III. The $E(\mathbf{k})$ vs $\mathbf{k}$ are listed. The first column gives the BSW symbol (where appropriate); the second column specifies $\mathbf{k}$ (see text); the third and alternate columns specifies the irreducible representation appropriate for that eigenvalue; the fourth and alternate columns give the energy eigenvalues in rydbergs. In order to obtain the correct energy for a given $\mathbf{k}$ the value of the constant potential between spheres (−0.939 Ry) must be added to the listed value. Thus, the first energy listed under "Band 1" corresponds to Γ_1 and is (−0.104−0.939) = −1.043 Ry. The italicized values were obtained by graphical interpolation.

		Conduction bands											
	k	Band 1		Band 2		Band 3		Band 4		Band 5		Band 6	
Γ	000	1	−0.10	25′	0.299	25′	0.299	25′	0.299	12	0.357	12	0.357
Δ	010	1	*−0.09*	2′	0.294	5	0.301	5	0.301	1	0.353	2	0.358
Δ	020	1	*−0.05*	2′	0.282	5	0.309	5	0.309	1	0.341	2	0.361
Δ	030	1	*+0.01*	2′	0.265	5	0.323	5	0.323	1	0.329	2	0.365
Δ	040	1	*0.08*	2′	0.243	1	0.328	5	0.342	5	0.342	2	0.371
Δ	050	1	0.148	2′	0.224	5	0.365	5	0.365	1	0.372	2	0.379
Δ	060	1	0.166	2′	0.210	5	0.388	5	0.388	2	0.390	1	0.483
Δ	070	1	0.164	2′	0.201	5	0.405	5	0.405	2	0.394	1	0.621
X	080	1	0.163	3	0.200	2	0.399	5	0.412	5	0.412	4′	0.704
Σ	110	1	*−0.08*	3	0.291	2	0.303	1	0.303	4	0.352	1	0.356
	120	+	−0.02	−	0.28	+	0.30	−	0.31	+	0.34	+	0.35
	130	+	0.05	−	0.264	+	0.31	−	0.323	+	0.33	+	0.36
	140	+	0.11	−	0.245	+	0.310	−	0.342	+	0.35	+	0.37
	150	+	0.157	−	0.227	+	0.327	−	0.365	+	0.37	+	0.41
	160	+	0.173	−	0.213	+	0.358	−	0.388	+	0.38	+	0.515
	170	+	0.171	−	0.204	+	0.38	+	0.39	−	0.405	+	0.651
Z	180	1	0.168	4	0.203	3	0.393	1	0.393	2	0.412	3	0.736
Σ	220	1	*0.00*	3	0.275	1	0.308	2	0.315	4	0.339	1	0.364
	230	+	*0.07*	−	0.264	+	0.30	−	0.325	+	0.33	+	0.38
	240	+	0.133	−	0.250	+	0.294	+	0.348	−	0.343	+	0.41
	250	+	0.183	−	0.236	+	0.295	+	0.364	−	0.365	+	0.47
	260	+	0.193	−	0.224	+	0.317	+	0.378	−	0.388	+	0.579
	270	+	0.188	−	0.217	+	0.340	+	0.38	−	0.405	+	0.721
Z	280	1	0.185	4	0.216	3	0.351	1	0.380	2	0.412	3	0.815
Σ	330	1	0.11	3	0.262	1	0.298	2	0.333	4	0.330	1	0.411
	340	+	0.174	−	0.257	+	0.283	−	0.346	+	0.335	+	0.46
	350	+	0.215	−	0.250	+	0.270	−	0.366	+	0.351	+	0.537
	360	+	0.219	−	0.243	+	0.280	−	0.388	+	0.361	+	0.658
	370	+	0.210	−	0.237	+	0.298	−	0.404	+	0.362	+	0.80
Z	380	1	0.205	4	0.237	3	0.307	2	0.412	1	0.363	3	0.921
Σ	440	1	0.212	3	0.264	1	0.272	4	0.332	2	0.355	1	0.523
	450	+	*0.22*	−	0.267	+	*0.26*	+	*0.34*	−	0.370	+	0.619
	460	+	0.23	+	0.25	−	0.268	+	0.35	−	0.388	+	0.751
	470	+	0.22	+	0.26	−	0.267	+	0.352	−	0.404	+	0.911
W	480	2′	0.216	3	0.268	3	0.268	1	0.354	1′	0.412	3	1.044
Σ	550	1	0.23	1	0.25	3	0.286	4	0.345	2	0.377	1	0.727
	560	+	0.22	+	0.24	−	0.298	+	0.354	−	0.391	+	0.863
	570	+	0.21	+	0.23	−	0.304	+	0.360	−	0.404	−	0.941
K	660	1	0.205	1	0.228	3	0.327	4	0.367	2	0.396	3	0.906
Λ	111	1	−0.065	3	0.305	1	0.289	3	0.353	3	0.305	3	0.353
	121	+	*+0.00*	+	0.27	−	0.309	+	0.30	−	0.35	+	0.34
	131	+	*0.06*	+	0.266	−	0.318	+	0.31	−	0.36	+	0.34
	141	+	0.11	+	0.248	−	0.333	+	0.305	−	0.37	+	0.373
	151	+	0.165	+	0.232	−	0.348	+	0.318	−	0.390	+	0.43
	161	+	0.179	+	0.21	−	0.367	+	0.348	−	0.40	+	0.538
	171	+	0.17	+	0.20	−	0.38	+	0.372	−	0.40	+	0.676
S	181	1	0.17	1	0.206	3	0.381	4	0.389	2	0.408	3	0.765
	221	1	*0.03*	+	0.27	+	0.30	−	0.31	−	0.34	+	0.36
	231		*0.09*		0.26		0.30		0.31		0.35		0.379
	241		0.139		0.258		0.297		0.329		0.370		0.411
	251		0.185		0.243		0.296		0.342		0.388		0.47
	261		0.19		0.230		0.315		0.360		0.400		0.59
	271		0.195		0.222		0.337		0.372		0.401		0.740
	281	+	0.191	+	0.218	−	0.345	+	0.375	−	0.405		
	331	+	*0.12*	+	0.27	+	0.29	−	0.316	−	0.35	+	0.40
	341		0.171		0.273		0.287		0.322		0.362		0.47
	351		0.206		0.260		0.280		0.336		0.381		0.542
	361		0.219		0.244		0.287		0.351		0.393		0.668
	371		0.215		0.239		0.299		0.359		0.401		0.823
	381	+	0.21	+	0.23	−	0.304	+	0.36	−	0.404	+	1.026
	441	+	0.198	+	0.27	+	0.28	−	0.322	−	0.366	+	0.523
	451		0.219		0.261		0.288		0.331		0.380		0.623
	461		0.236		0.242		0.283		0.343		0.391		0.755
Q	471	−	0.226	+	0.252	−	0.276	+	0.352	+	0.401	−	0.897
	551	+	0.22	+	0.25	+	0.29	−	0.335	−	0.385	+	0.727
	561		0.222		0.243		0.299		0.347		0.393		0.832
Λ	222	1	0.05	1	0.281	3	0.309	3	0.309	3	0.359	3	0.359
	232	+	*0.11*	+	0.28	−	0.309	+	0.30	−	0.374	+	0.36
	242	+	0.150	+	0.27	−	0.315	+	0.29	−	0.389	+	0.41
	252	+	0.188	+	0.258	−	0.326	+	0.296	−	0.399	+	0.507

TABLE III (*continued*).

	k	Band 1		Band 2		Band 3		Band 4		Band 5		Band 6	
	262	+	0.70	+	0.241	−	0.342	+	0.30	−	0.403	+	0.63
	272	+	0.20	+	0.23	−	0.357	+	0.321	−	0.400	+	0.790
U	282	1	0.20	1	0.228	3	0.327	4	0.367	2	0.396	3	0.904
	332	+	0.132	+	0.30	−	0.305	+	0.30			+	0.398
	342		0.165		0.291		0.306		0.314		0.383	+	0.46
	352		0.193		0.272		0.306		0.320		0.396		0.550
	362		0.212		0.253		0.302		0.332		0.400		0.691
	372		0.222		0.242		0.299		0.347		0.393		0.832
	442	+	0.180	+	0.285	−	0.307	+	0.330	−	0.384	+	0.522
	452		0.197		0.272		0.315		0.321		0.392		0.623
Q	462	+	0.216	−	0.256	+	0.329	−	0.303	+	0.395	−	0.728
	552	+	0.204	−	0.320	+	0.265	−	0.396	+	0.315	+	0.686
Λ	333	1	0.147	3	0.301	3	0.301	1	0.366	3	0.386	3	0.386
	343	+	0.165	−	0.233	+	0.294	+	0.360	−	0.350		
	353	+	0.183	+	0.281	−	0.308	+	0.337	−	0.401		
	363	+	0.204	+	0.265	−	0.320	+	0.315	−	0.396	+	0.686
	443	+	0.168	+	0.293	−	0.300	+	0.377	−	0.396	+	0.516
Q	453	+	0.179	−	0.284	+	0.305	−	0.353	+	0.400	−	0.587
L		1	0.164	3	0.297	3	0.297	3	0.401	3	0.401	2′	0.510

$E(k)$ for the excited bands

	k	Band 7		Band 8		Band 9		Band 10		Band 11		Band 12	
Γ	000	2′	2.271	15	*2.36*	15	*2.36*	25′	2.634	25′	2.634	25′	2.634
Δ	010	5	2.300	5	2.300	2′	2.233	1	2.352	1	2.867	2′	2.719
Δ	020	5	2.134	5	2.134	2′	2.152	1	2.247	1	2.623	2′	2.887
Δ	030	5	1.974	5	1.974	2′	2.075	1	2.126	1	2.344		
Δ	040	5	1.830	5	1.830	1	1.931	2′	2.015	1	2.168		
Δ	050	1	1.672	5	1.708	5	1.708	2′	1.970	1	2.097		
Δ	060	1	1.417	5	1.614	5	1.614	2′	1.940	1	2.063		
Δ	070			5	1.554	5	1.554	2′	1.923				
X	080	1	1.091	5′	*1.54*	5′	*1.54*	3	1.915	1	2.042		
Σ	110	3	2.117	1	2.162	3	2.368	4	2.445	2	2.657	1	2.683
	120	−	1.97	+	2.005	+	2.378						
	130	−	1.845	+	1.863	−	2.225						
	140	−	1.723	+	1.736	+	1.959	−	2.142	+	2.265		
	150	−	1.616	+	1.63	+	1.69	−	2.081				
	160	+	1.428	−	1.533	+	1.550	−	2.037				
	170	+	1.209	+	1.497	−	1.480	−	2.02				
Z	180	1	1.096	4	1.460	1	1.478	4	2.006	1	2.126	2	3.51
Σ	220	3	1.823	1	1.850	3	2.449	1	2.50	4	2.54	2	2.695
	230	−	1.690	+	1.713	−	2.428	−	2.840				
	240	−	1.569	+	1.593	+	1.98						
	250	−	1.467	+	1.550	+	1.718						
	260	−	1.388	+	1.42	+	1.46						
	270	+	1.233	−	1.340	+	1.38						
Z	280	1	1.113	1	1.371	4	*1.30*	1	2.318	4	*2.32*	1	3.498
Σ	330	3	1.551	1	1.579	1	2.321	4	2.334	3	2.592	4	2.722
	340	−	1.427	+	1.469								
	350	−	1.327	+	1.385	+	1.770						
	360	−	1.248	+	1.33	+	1.513						
	370	−	1.196	+	1.27	+	1.29						
Z	380	1	1.145	4	1.180	1	*1.27*	4	*2.41*	1	*2.61*		
Σ	440	3	1.305	1	1.370	4	2.082	1	2.173	3	2.805	2	2.889
	450	−	1.200										
	460	−	1.116	+	1.241	+	1.588	+	2.37				
	470	−	1.064	+	1.209	+	1.354						
W	480	3	1.044	2′	1.184	1	1.212	3	2.672	2′	2.709		
Σ	550	3	1.08	4	1.862								
	560	−	1.02	+	1.181	+	1.666						
	570	+	1.026	+	1.14	+	1.444						
K	660	1	0.998	1	1.125	4	1.688	1	2.009	1	2.693		
Λ	111	1	1.968	1	2.300	3	2.332	3	2.332	1	2.750	3	2.769
	121	+	1.814										
	131	+	1.674	−	2.02								
	141	+	1.554	+	1.95	−	1.858						
	151	+	1.457	+	1.694	−	1.739	+	2.02				
	161	+	1.38	+	1.440	−	1.650	+	1.99				
	171	+	1.217	+	1.332	−	1.591	+	1.97				
S	181	1	1.103	1	1.315	4	1.574	1	1.972	1	2.258		
	221	+	1.656	+	2.02								
	231		1.515		1.900								
	241		1.42		1.78		2.02						
	251		1.302		1.66		1.74						

TABLE III (*Continued*).

	k	Band 7		Band 8		Band 9		Band 10		Band 11		Band 12	
	261		1.226		1.47		1.606						
	271		1.19		1.27		1.557						
	281	+	1.10	+	1.18	+	1.541						
	331	+	1.379	+	1.771								
	341		1.262		1.657								
	351		1.168		1.58		1.78						
	361		1.096		1.50		1.54						
	371		1.05		1.29		1.457						
	381	+	1.15	+	1.444								
	441	+	1.147	+	1.548								
	451		1.06		1.464		1.852						
	461		0.984		1.42		1.598						
Q	471	+	0.958	−	1.361	+	1.370						
	551	+	0.963	+	1.382	−	1.870						
	561		0.923										
Λ	222	1	1.496	1	2.241	3	2.248	3	2.248	3	2.676	3	2.676
	232	+	1.354										
	242	+	1.240	−	1.947	+	2.02						
	252	+	1.144	+	1.754	−	1.834						
	262	+	1.06	+	1.501	−	1.752						
	272	+	1.023	+	1.275	−	1.702	+	2.02				
U	282	1	0.998	1	1.145	4	1.688	1	2.009	1	2.693		
	332	+	1.220	+	1.98								
	342		1.105		1.876								
	352		1.02		1.78		1.82						
	362		0.946		1.555		1.725						
	372		0.923		1.327		1.683						
	442	+	0.993	+	1.777								
	452		0.914		1.70		1.886						
Q	462			−	1.626	+	1.646	−	2.305	+	2.602		
	552	+	0.875	+	1.615	−	1.913						
Λ	333	1	1.085	1	2.163	3	2.198	3	2.198	3	2.504	3	2.504
	343			+	2.09	−	2.09		2.16		3.285		
	353	+	0.898	+	1.863	−	1.98						
	363	+	0.874			−	1.913						
	443	+	0.886	+	2.02								
Q	453	+	0.854	−	1.916	+	1.958	−	2.196	−	2.709	+	3.000
L	444	1	0.845	2′	2.130	3	2.441	3	2.441	1	2.804		

Some additional $E(\mathbf{k})$ of high energy

	k	Band 13		Band 14		Band 15		Band 16		Band 17	
Δ	010	5	2.758	5	2.758						
Δ	020	5	2.937	5	2.937						
Σ	110	3	2.898	4	2.95						
Σ	220	1	3.054	3	3.184	1	3.413	3	3.446	1	3.70
Σ	330	2	2.771								
Λ	111	3	2.769	3	2.769	3	2.980	3	2.980		
Λ	222	1	2.775								
Λ	333	1	2.804								
Q	453	+	3.519	−	3.518						

Note that there are three points "like" $X(080)$ whereas there are six such points shown in Fig. 2 (viz., the center of each of the square faces). The reason for this is that each of these six points is shared with an adjoining Brillouin zone and, therefore, only three belong to the first zone. In general, the number of "like" points can be obtained by dividing 48 (the order of the cubic group) by the order of the group of the wave vector. This rule is valid for all points except those on the hexagonal faces, the reason for this being that these surfaces are arbitrary to a certain extent (see reference 22). Of course, the sum of all the entries under "No. of like vectors" should be 2048, which it is.

Parameters of the Calculation

Slater's atomic units (a.u.) have been used throughout unless otherwise stated. Thus, the unit of energy is the rydberg and the unit of dimension is the Bohr radius:

$$\begin{aligned} &1 \text{ rydberg (Ry)} = 13.605 \text{ eV}, \\ &1 \text{ Bohr radius} = \hbar^2/me^2 = 0.529171 \text{ Å}. \end{aligned} \tag{16}$$

The lattice constant for copper was taken to be

$$a = 3.6147 \text{ Å} = 6.83087 \text{ a.u.} \tag{17}$$

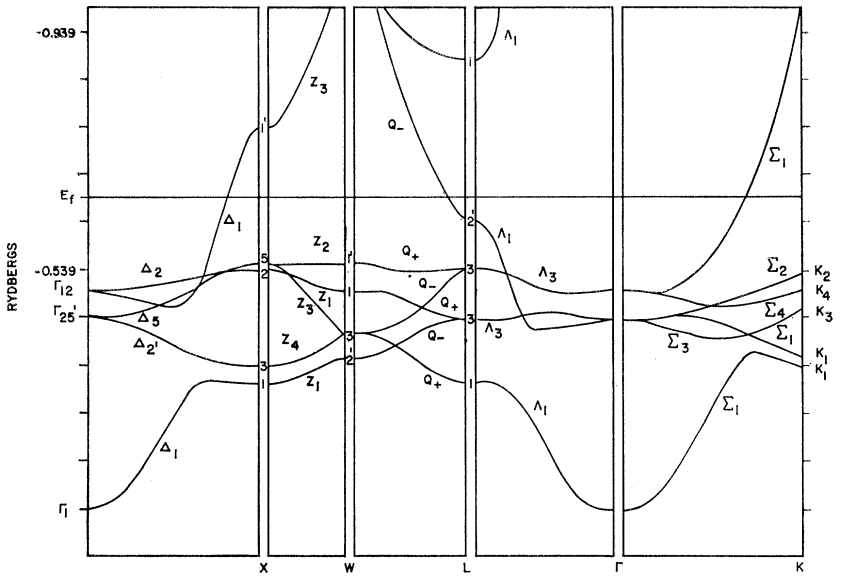

FIG. 3. Energy bands for copper using Chodorow's potential.

This is the value measured by Frohnmeyer and Glocker[23] in 1953.

The "sphere radius" R was taken to be half the nearest-neighbor distance. Hence,

$$R=\sqrt{2}(a/4)=2.4151 \text{ a.u.} \tag{18}$$

The quantity π/a is now easily determined and is

$$\pi/a=0.459911 \text{ a.u.} \tag{19}$$

Energy Eigenvalues

The energy versus $\mathbf{k}$, $E(\mathbf{k})$, was computed for the equivalent of 2048 points of the Brillouin zone. These calculations were carried out for the six bands "at" and immediately below the Fermi energy (the band "at" the Fermi energy being the conduction band and is half "full") and for energies up to 2 Ry above the Fermi energy. For certain points of high symmetry the calculations were made for still higher energies. The results of these calculations are tabulated in Table III. A plot of the energy bands is shown in Figs. 3 and 4. Figure 3 gives the detailed structure for energies near the Fermi energy, whereas Fig. 4 is a plot on a condensed energy scale in order to show the excited bands. The bands are labeled in a manner consistent with Eq. (15) where the band containing the state arising from the $4s$ electrons located at $\mathbf{k}=(0,0,0)$ (which is the Γ_1 state) is defined as the first band. The bands are then numbered consecutively as one increases in energy for fixed $\mathbf{k}$.

The critical consideration at this point is one of convergence. For our purposes, we say that convergence has been obtained if a given energy eigenvalue is unaffected when an arbitrary increase is made in the number of l values and/or the number of $\mathbf{k}_i$ used in the expression of the APW's and the wave function, respectively; "unaffected" means that the eigenvalue did not change within the accuracy being sought. From previous work in the SSMTG it has been shown that convergence is attained if one uses the first five l values ($=0, 1, 2, 3, 4$) and all $\mathbf{k}_i$ for which $k_i^2 \leq 40\pi^2/a^2$. Under these conditions an accuracy to better than 0.01 Ry can be expected. This is in accord with what the author has found. Doubling the number of l and $\mathbf{k}$ values used, either separately or simultaneously, never changed the eigenvalues by more than 0.005 Ry.

The Fermi Energy

Periodic boundary conditions have been used. This restricts the allowable $\mathbf{k}$ values to a uniformly distributed discrete set in reciprocal space, containing N allowable $\mathbf{k}$ values in each Brillouin zone where N represents the number of unit cells in the solid being considered. Each $\mathbf{k}$ state can accommodate two electrons, one with spin up the other with spin down. Now, recall that the nth energy band can be defined as the set of all energies $E_n(\mathbf{k})$ obtained as $\mathbf{k}$ ranges over all permissible values in the nth Brillouin zone. In the reduced zone scheme this amounts to fixing n (that is the particular branch of energy values) and allowing $\mathbf{k}$ to range over all permissible values of the first Brillouin zone. Hence, a given energy band can accommodate two electrons from each atom in the solid.

In the case of copper, the bands arising from the $1s$, $2s$, $2p$, $3s$, and $3p$ levels of the atom lie considerably below the conduction band and, consequently, will be completely occupied. This being the case, we need consider only the bands arising from the $4s$ and $3d$ atomic states. Hence, the computed bands must ac-

[22] L. P. Bouchaert, R. Smoluchowski, and E. Wigner, Phys. Rev. **50**, 58 (1936); hereafter referred to as BSW.
[23] G. Frohnmeyer and R. Glocker, Acta Cryst. **6**, 19 (1953).

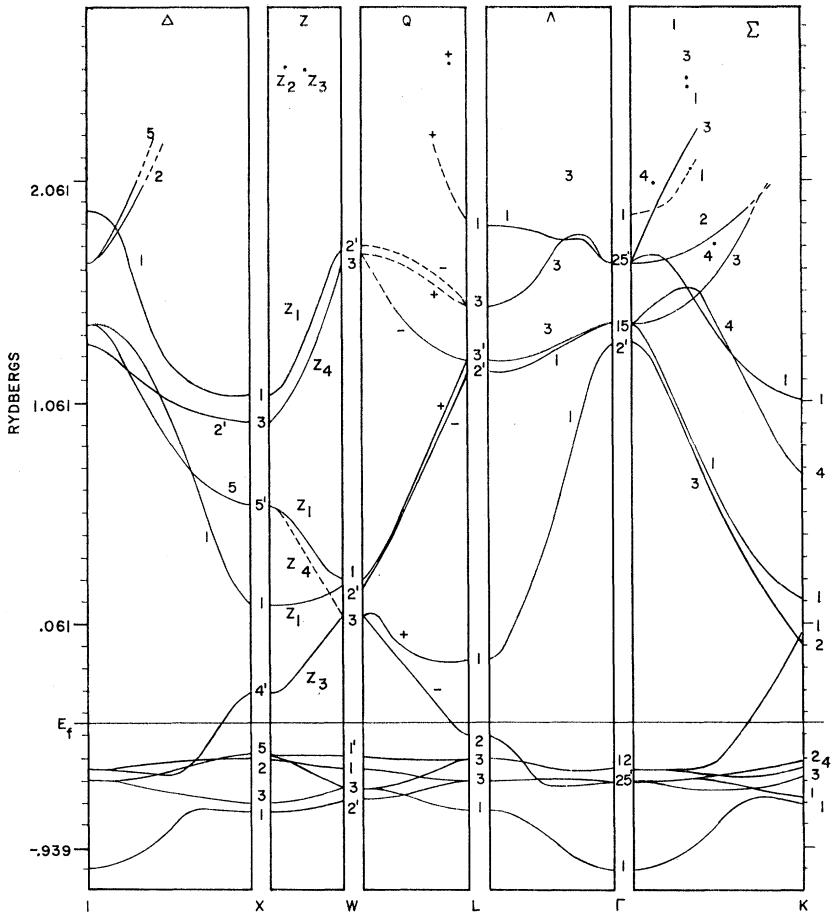

FIG. 4. Energy bands for copper using Chodorow's potential—high-energy region.

commodate eleven electrons from each atom; ten 3*d* electrons and one 4*s* electron.

The procedure used to determine the Fermi energy is the following. The 89 energies listed for each band in Table III, in reality, represent 2048 energies as discussed earlier. The number of times that an energy corresponding to a given **k** is to be counted is given in Table II under the heading "No. of like vectors." Taking this into account, we start with the lowest energy and label it number one, the next lowest and label it

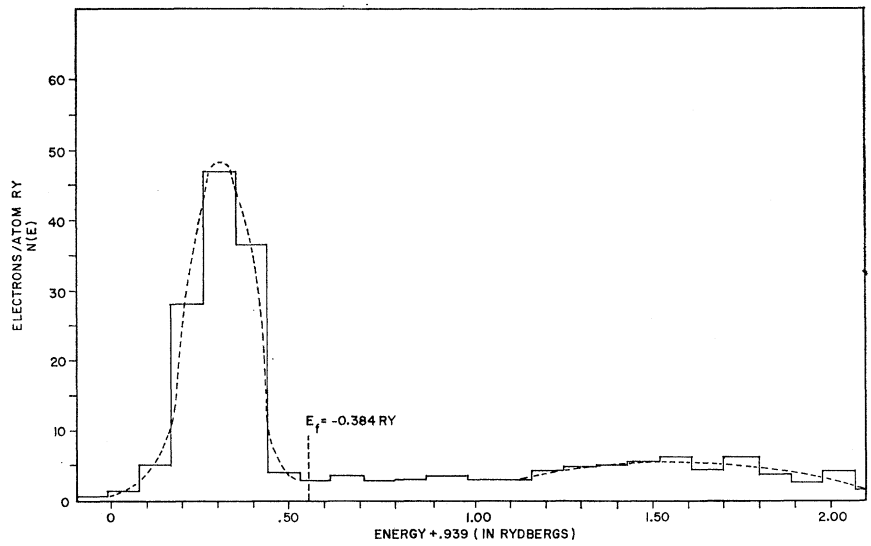

FIG. 5. Histogram for the density of states.

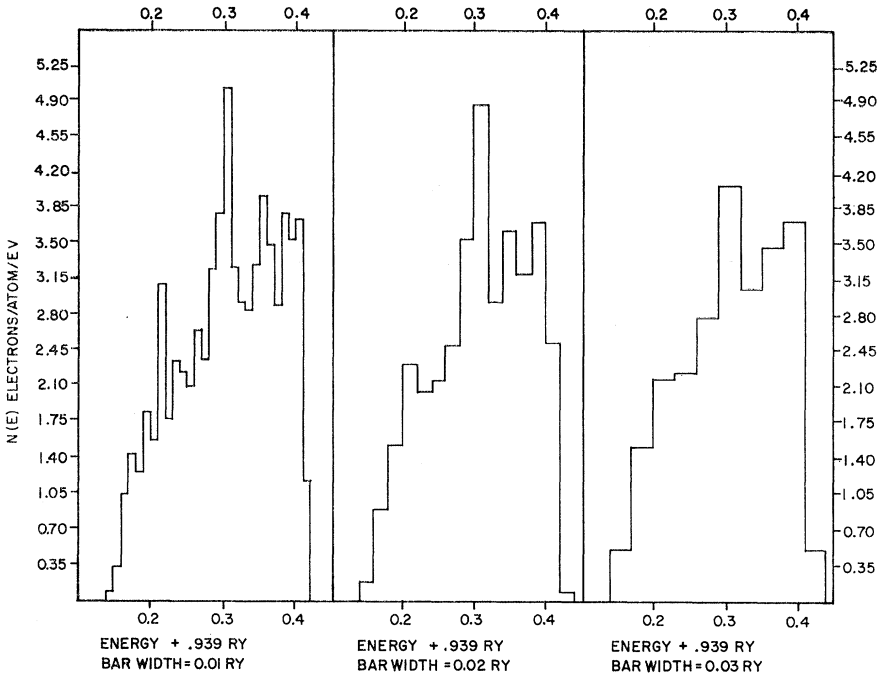

FIG. 6. Fine structure of "*d*-hump."

number two, and so on until we have exhausted the list of energies. Assuming that each such energy is the average for all $E(\mathbf{k})$ from the same volume element, the first (5.5) (2048) = 11 264 energies will be occupied and all higher energies will be unoccupied. It therefore follows that the Fermi energy, in this approximation, lies somewhere between energy number 11 264 and energy number 11 265.

It so happens that both energies have the same value of −0.384 Ry. We thus have

$$\text{Fermi energy} = E_f = -0.384 \text{ Ry}. \tag{20}$$

The Density of States

The density of states is defined as the number of energy states per unit volume per unit energy range. Thus the number of states per unit volume of the crystal having energies in the range E to $E+dE$ is given by

$$N(E) = n(E)dE, \tag{21}$$

where $n(E)$ is the density of states.

The $n(E)$ curve was obtained in the following way. A ΔE was chosen, then the energy scale was partitioned into intervals by the points $E+n(\Delta E)$ for $n=0$, 1, 2, 3, $\cdots$. The number of computed energy values lying within the first interval was determined, then a bar with height proportional to this number was plotted in the interval. The process was then repeated for the second interval and so on, until all energy values were exhausted. The value of ΔE was then increased and the entire process repeated. This was done until the histogram did not change its form appreciably from one ΔE to the next. A smooth curve was then drawn using the final histogram as a guide. The curve was made to pass through the midpoint of the top of each bar except for regions where such a procedure gave unrealistically rapid fluctuations.

The "stable" histogram was one which had a $\Delta E = 0.09$ Ry. This histogram and the resulting density of states curve are shown in Fig. 5. A much smaller ΔE can be used over the region of the "*d* hump" where the eigenvalues are heavily concentrated. Figure 6 shows a series of histograms for this region which suggest that considerable fine structure is present in the "*d* hump."

The Fermi Surface

The Fermi surface is given implicitly by the equation

$$E(k) = E_f = -0.38 \text{ Ry}.$$

This equation was solved graphically by plotting $E(\mathbf{k})$ versus $\mathbf{k}$ in various directions. It was then an easy matter to establish those points $\mathbf{k}_f$ on the Fermi surface

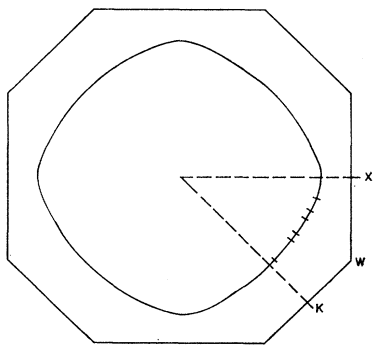

FIG. 7. (100) cross-section of the Fermi surface.

from the intersection of the line $E=E_f$ with the $E(\mathbf{k})$ curve. This procedure was carried out for enough $\mathbf{k}_f$ to enable a fairly accurate determination of the E_f contours of constant energy in three planes; the ⟨100⟩ plane, the ⟨110⟩ plane, and the plane containing the hexagonal face. These contours for E_f are shown in Figs. 7, 8, and 9, respectively.

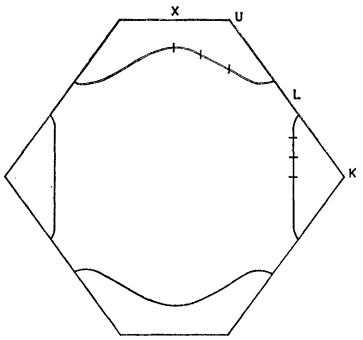

FIG. 8. (110) cross section of the Fermi surface.

Points on the contours which were actually determined are marked by small circles, or by short straight lines. The possible errors involved have been indicated by the length of the lines.

The striking features of the Fermi surface (as have been pointed out earlier[24,25]) are:

(1) The "belly" region deviates quite significantly from being spherical. It is somewhat protruded ("egg shaped") in the ⟨100⟩ direction and contracted in the ⟨110⟩ direction.

(2) The Fermi surface touches the edge of the zone over a relatively large region at the center of the eight hexagonal faces. The portion of the surface extending in these directions (the ⟨111⟩ directions) are referred to as the "necks" in the literature.

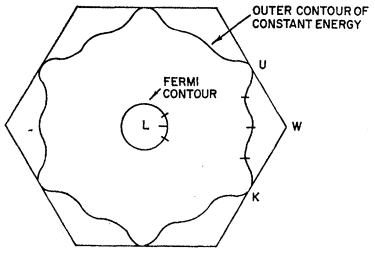

FIG. 9. Intersection of Fermi surface with hexagonal face.

(3) On the hexagonal face, the outer contour of constant energy presents a very striking "cookie cutter" like shape (see Fig. 9). Calculations indicate that the Fermi surface contour on this face may also be of the "cookie-cutter" shape but possible error prohibits a definite choice between a "cookie-cutter" contour and a circular contour.

[24] B. Segall, Phys. Rev. Letters 7, 154 (1961).
[25] Glenn A. Burdick, Phys. Rev. Letters 7, 156 (1961).

The Fermi surface, as computed, here was compared with Morse's experimentally determined Fermi surface and found to be in excellent agreement.[25] More recent experiments by Bohm and Esterling[26] indicate a Fermi surface which is (within stated possible errors) identical to the author's in the parameters available for comparison.

DISCUSSION OF RESULTS AND COMPARISON WITH EXPERIMENTS

As stated earlier, Segall calculated the $E(\mathbf{k})$ for copper using the Green's function method. He used Chodorow's potential (as well as a modified Chodorow potential) and calculated the $E(\mathbf{k})$ only along various symmetry lines and at points in the (110) plane. The author's corresponding values agree with Segall's within 0.01 Ry in practically all cases. Although the potentials used by Segall and the author were both essentially Chodorow's original one, there were slight differences. To check the effect of these differences, Segall used exactly the author's potential to calculate the $E(\mathbf{k})$ at a few points of high symmetry.[27] Table IV compares these points with the authors.

TABLE IV. Comparison of APW and Green's function solutions of Schrödinger's equation (energy in rydbergs).

Point	APW (Burdick)	Green's function (Segall)
X_1	−0.776	−0.771
X_3	−0.739	−0.738
X_4'	−0.234	−0.233
L_1	−0.775	−0.773
L_3	−0.642	−0.644

The remarkable agreement illustrated by Table IV strongly suggests that an accurate solution of Schrödinger's equation for the potential used has been achieved by both parties. In every case where both parties calculated a particular physical quantity using Chodorow's potential, they were in close agreement. For example, Segall reports an E_f of -0.385 ± 0.010 Ry; the author's is −0.384 Ry. The fact that the author's Fermi energy and Fermi surface are in such good agreement with Segall's indicates that the approximations made by Segall are quite good. Segall did not compute a sufficient number of $E(\mathbf{k})$ to make a straightforward determination of E_f or the density of states possible.

Density of States vs Soft X-Ray Absorption and Emission

The absorption of x rays incident on a metal will pass through various maxima as the frequency is increased. These maxima will correspond to lifting electrons from

[26] H. V. Bohm and V. J. Esterling, Bull. Am. Phys. Soc. 6, 438 (1961); H. V. Bohm (private communication).
[27] B. Segall (private communication).

the various low-lying bands up to the first unoccupied states which occur in the conduction band. Thus, as the frequency of the incident x-rays is increased, we pass through the absorption edge and on into the fine structure of the absorption. The sudden increase in absorption at the "edge" is because at this frequency the x-ray photons have just enough energy to "lift" electrons from one of the low-lying bands up to the Fermi energy; since the electron energies in these lower bands are nearly independent of $\mathbf{k}$ (these bands are said to be flat), all electrons in the band suddenly become available to the absorption process, thus resulting in a sudden increase (the absorption edge) in the absorption of x rays. The photon energy at which the absorption edge occurs should therefore be the energy separation of the band in question and the Fermi energy. That is, the absorption edge gives the Fermi energy relative to that band which gives rise to the "edge." This identification of the absorption edge will allow us to compare features of our calculated density of states curve with the fine structure of the absorption vs photon energy curve. To make these comparisons we shall assume that the transition probability for the bands in question is a slowly varying function of the energy. If this is the case, the fine structure of the absorption curve should reproduce the general features of our density of states curve in the region just above the Fermi energy.

TABLE V. Energy in eV.

	Beeman and Friedman	Burdick	Rudberg and Slater
E_D	−3.4	−3.4	−3.6
E_C	−1.9	−1.9	−2.1
E_F'	−0.2	···	···
E_M	4.0		3.4
E_A	14.7	14.5	12.2
E_G	19.4	20.9	17.2
E_B	24.1	···	21.7

The x-ray emission in metals occurs when some of the states in the low-lying bands have been vacated by some mechanism. Once vacant states are available in these bands then electrons in the conduction band can drop into the available "holes" thus giving rise to x-ray emission. A study of the emission spectra should therefore give us information about the density of states just below the Fermi energy. In particular, the emission spectra should confirm the general shape of the large "hump" in our density of states curve if this "hump" is really there; of course, it is again assumed that the transition probability is approximately constant in this region.

Beeman and Friedman (17) made x-ray absorption and emission measurements on copper and, as stated in the introduction, compared their results with a density of states curve obtained by Rudberg and Slater.[16] We now compare our density of states with Beeman's work. Figures 10(a), 10(b), and 10(c) show Beeman's absorption curve, Slater's density of states, and the author's density of states, respectively. Beeman and Friedman attempted to correlate certain points of their absorption and emission curves for the K shell with points on Rudberg and Slater's density of states. "Corresponding" points for the three have been labeled with the same letter in the respective figures. The points in Figs. 10(a) and 10(b) were located from data given in reference 17. The energy scales have been shifted to make the points labeled F (Fermi energy) have the same energy; this energy has been arbitrarily set equal to zero. The energies of the various points relative to the Fermi energy are tabulated in Table V for the three cases.

The most striking difference in the two density-of-states curves is the "camel" hump which appears in Fig. 10(b) but not in Fig. 10(c). The x-ray emission

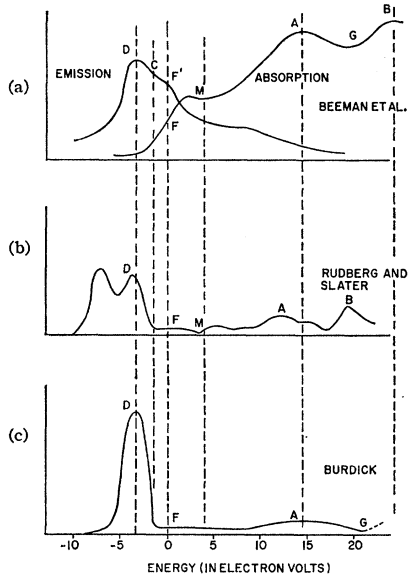

FIG. 10(a). K-band absorption and emission spectra for copper (from Beeman *et al.*). (b) Rudberg and Slater's density of states for copper. (c) Burdick's density of states for copper.

curves measured for various bands indicate that the shape of this portion of the density of states is more nearly like that of Fig. 10(c). Perhaps a point of greater surprise should be the general likeness of Figs. 10(b) and 10(c) in view of the limited data available at the time Rudberg and Slater did their work. The two curves are in remarkable agreement with respect to E_D and E_C. Furthermore, the shape and height of the density of states in the immediate neighborhood of E_F are in agreement. The two curves were brought to the same vertical scale by requiring the areas under the curves for $E \leq E_F$ to be the same.

The minimum at M in Fig. 10(a) is missing in Fig. 10(c). A possible explanation for this minimum is the following. The energy-band plot of Fig. 3 indicates that

the wave functions are mostly p like (e.g., this is the symmetry of L_2') in the neighborhood of the Fermi energy, changing to mostly s like (e.g., L_1) about 4 eV above the Fermi energy. Recalling that we are considering transitions from a state of s-like symmetry (K shell) we should expect a large reduction in transition probability about 4 eV above the Fermi energy. Thus, the dip at M is probably due not to a decrease in the density of states but mainly to a fairly large decrease in transition probability. It is interesting to note that the energy of L_1 minus the Fermi energy is 4.0 eV agreeing surprisingly well with E_M-E_F of Beeman and Friedman's work which is also 4.0 eV. If the minimum is due primarily to the decrease in transition probability (as the above would suggest) then we should observe maxima at this point in case of L_2 or M_2 absorption which has p symmetry. The above interpretation of the minimum at M would also provide a possible explanation for the high energy satellite observed in the $M_{2,3}$ emission spectrum as determined by Bedo and Tomboulian.[28] In their measurements, a secondary maximum in the emission occurs 7.4 eV above the principal maximum (see Table 1, p. 466, reference 28). If we say that the principal maximum corresponds to D in Fig. 14 (which it certainly must) then, the second maximum occurs 4.0 eV (=7.4−3.4) or at precisely the point where we said that the eigenfunctions become mostly s like.

Bedo and Tomboulian's work would indicate that the "d hump" in our density of states should occur about 5.0 eV below the Fermi energy. This value does not agree nearly so well with the theoretical value as does Beeman and Friedman's value.

The emission curve in Fig. 10 is in remarkable agreement with the author's density of states. The emission intensity is comparatively constant in the interval E_C to E_F corresponding to a "flat" density of states in this interval. A sharp drop in emission occurs at E_F agreeing very well with the sudden decrease in the percentage of levels occupied as one goes above the Fermi energy. (There will be a number of higher levels occupied as a result of "kicking" the K electrons up to higher levels, or out of the metal, in order to obtain the necessary vacant states in the K shell. This contributes to the long high-energy tail of the emission curve.) One might think that the emission intensity at D should be much larger than it is and if the transition probability were constant it certainly would be. We must remember, however, that the levels in the vicinity of D are mostly of "d"-like symmetry and, therefore, there will be a strong quenching of the "d hump" in the K-emission spectra.

[28] D. E. Bedo and D. H. Tomboulian Phys. Rev. **113**, 464 (1959).

Optical Data

Roberts[29] has measured the absorption of electromagnetic radiation in the optical region by reflectivity measurements. He measures a minimum in the absorption at 0.65 μ and a diffuse relative maximum at approximately 0.50 μ. These values correspond to energies of 1.9 and 2.5 eV, respectively; the half maximum corresponds to an energy of 2.2 eV and is the value referred to in the literature as the "well-known" interband transition of copper. Now, the 1.9 eV should correspond to the author's value of E_F-E_C which was computed to be 1.9 eV. The 2.5 eV should correspond to E_F-E_D which was computed to be 3.4 eV.

It is interesting to note that Segall[15] attributed the 2.2-eV value to transitions from the d state around L_3 to the p state at the Fermi energy. He obtained a value of 2.6 eV using his modified potential and a value of 2.1 eV using Chodorow's potential. The author's corresponding value is 2.2 eV. The fact that the latter value agrees precisely with that obtained from the density of states and that obtained by Roberts is fortuitous. This is to say, there is no reason for them to be in more than qualitative agreement.

SUMMARY

A thorough energy band calculation has been carried out for copper using Chodorow's potential for d electrons and Slater's APW method. The computations were done on a high-speed digital computer using a program due to Wood.

The $E(k)$ values were computed for the equivalent of 2048 points in the Brillouin zone and for energies ranging from the bottom of the 4s band to approximately 2 Ry above the Fermi energy. From these calculations the Fermi energy, Fermi surface, and density of states were determined. Comparison of results with experiment has shown not only qualitative but in most cases quantitative agreement. Agreement with independent theoretical work by Segall suggests that an accurate solution of Schrödinger's equation using Chodorow's potential has been obtained.

ACKNOWLEDGMENTS

It is with pleasure that the author acknowledges his indebtedness to Dr. M. I. Chodorow for the potential used, Dr. J. H. Wood for the computer program and various discussions, Professor G. F. Koster for various discussions, and Professor J. C. Slater under whose direction this work was carried out. He further expresses his appreciation to Dr. B. Segall for his free exchange of unpublished data and to Mrs. Azzie Thomas for her preparation of the manuscript.

[29] S. Roberts, Phys. Rev. **118**, 1509 (1960).